ARCHIVES OF TRANSPORT *ISSN (print):* *0866-9546*
Volume 70, Issue 2, 2024 ***e-ISSN (online):*** *2300-8830*
DOI: *10.61089/aot2024.hc8s5k97*

SIMULATION AND ANALYSIS OF OPTIMAL ENERGY-SAVING MODE IN MICROFIELD OF UNDERGROUND RAIL TRANSIT

Shuang WU[1], Yunlan CHEN[2], Xin LIN[3]

[1, 3] *Department of Transportation Engineering, Yangzhou Polytechnic Institute, Yangzhou, China*

[2] *School of Transportation, Jilin Railway Technology College, Jilin, China*

Abstract:

Underground rail transit has become one of the most popular transportation modes because of its advantages such as fast running speed, large passenger flow and punctuality. This mode of transportation can alleviate urban traffic congestion to a certain extent, so underground rail transit has been vigorously developed, and the number of rail lines has increased exponentially. However, with the continuous development of underground rail transit, the energy consumption of train operation is also increasing, resulting in a waste of energy. To solve this problem, this paper proposes to improve the energy-saving technology of train operation by using train autopilot control strategy. Firstly, a train operation optimization model considering train position and speed limit is established by using automatic train driving strategy, and the nonlinear problem of the optimization model is solved by genetic algorithm. The micro-field theory is introduced into the control strategy of automatic train driving, and the energy-saving model of underground rail transit is established. The energy consumption is optimized from three aspects: train energy-saving technology, line planning and overall operation planning of rail transit. The simulation results show that the average impact rate and energy consumption of trains under the proposed energy-saving model are significantly reduced compared with the other two groups of trains, and the average impact rate and energy consumption are significantly reduced compared with the other two groups of trains. The running time and energy consumption of the energy-saving model are lower than those of the experimental group. To sum up, the energy-saving model of underground rail transit proposed in this paper not only reduces the operating energy consumption, but also improves the passenger comfort, which can provide low-cost energy-saving technology for underground transportation field, and has positive significance for urban low-carbon development.

Keywords: *underground rail transit, field theory, Automatic train driving, energy-saving model*

To cite this article:

Wu, S., Chen, Y., Lin, X., (2024). Simulation and analysis of optimal energy-saving mode in microfield of underground rail transit. Archives of Transport, 70(2), 27-42. https://doi.org/10.61089/aot2024.hc8s5k97

Contact:
1) 17327731310@163.com [https://orcid.org/0009-0006-6406-6510] - corresponding author, 2) w15052387587@126.com [https://orcid.org/0009-0003-2415-3095], 3) ADoversea@163.com [https://orcid.org/0009-0003-7642-6454]

1. Introduction

Currently, urban transportation congestion has become much worse, and underground rail transportation has somewhat reduced road congestion since it first appeared [Zhan et al., 2021]. Due to the advantages of large capacity, speed and convenience, underground rail transit has gradually become one of the preferred ways for people to travel [Yang et al., 2020]. However, with the continuous development of underground rail transit lines, its operation energy consumption is also increasing. The annual energy consumption of a medium-sized city is equivalent to the annual electricity consumption of 1 million households of three [Zhu et al., 2021]. This huge energy consumption not only increases the operating cost of underground rail transit, but also increases the burden on urban environmental management and increases the consumption of resources [Wen et al., 2020; Xu et al., 2021]. To solve the problem of excessive energy consumption of underground rail transit, this study proposes to use automatic train driving control strategy to change the energy consumption of rail trains during operation, so as to reduce the energy consumption of trains during operation. The strategy builds an energy-saving model of underground rail transit with the help of Microfield theory, and optimizes energy consumption from three aspects: train energy-saving technology, route planning and overall operation planning of rail transit. It is hoped that the model can enable underground rail transit to achieve an optimal energy-saving operation mode. The first part of this study is a brief introduction to the research on the development of underground rail transit in recent years and the application of automatic train driving technology. The second part introduces the method of using automatic train driving control strategy to achieve energy-saving in train operation, as well as the specific process of establishing an energy-saving model for underground rail transit using micro field theory. The third part verifies the practical effect of the proposed energy-saving model of underground rail transit through simulation experiments, and describes the experimental results. The last part is the analysis and summary of all the contents of this study. The research needs to solve the issue of how to reduce the energy consumption of underground rail transit and improve the travel comfort of passengers by optimizing train operation technology and operation planning. Specifically, how to improve the energy-saving technology of train operation through automatic driving control strategy; How to use field theory to build energy saving model of underground rail transit; How to optimize energy consumption from three aspects: train energy-saving technology, line planning and overall operation planning of rail transit.

2. Related work

Underground rail transit can not only alleviate urban traffic congestion, but also provide great convenience for people's travel, so many scholars have applied many high and new technologies in the development of underground rail transit. Vickerstaff et al. [2020] proposed a lifetime track prediction model based on circular drawing technology to solve the problem that the track interface of London Underground was prone to damage. Through empirical analysis, the model could accurately observe the damage of the track interface, thereby improving the accuracy of the predicted value of rolling contact fatigue damage. To solve the problem of high construction cost of underground rail transit, Cai and Chen [2021] proposed an independent covering geometric shell model to simulate fabricated lining. Through empirical analysis, the model could realize the automatic calculation of some engineering quantities and reduce the user cost of geotechnical engineers. Boyacioglu et al. [2022] proposed a wheel wear model integrating mechanics theory to solve the problem of high maintenance cost of rail train wheels. Through comparative tests, the model could make the repaired wheel more wear-resistant, reduce the number of wheel maintenance, and achieve the purpose of reducing maintenance costs. The Kong team [2020] proposed a switch based on group perception to solve the problem that the signal of the vehicle-passenger network is poor during the operation of underground rail trains. Through simulation experiment analysis, the switch could accurately describe the signal distribution and always recommend the best operator for users to connect. Hou et al. [2020] proposed an evaluation index and threshold method for platform noise of underground stations to accurately detect the noise of underground railway trains during operation. Through comparative test analysis, this method could effectively observe the noise in train operation.

Automatic train driving technology has provided a great contribution to the development of rail transit.

Feng et al. [2020] suggested a train speed trajectory optimization model based on notch selection and automatic train driving system to handle the issue of train speed optimization in intelligent high-speed railway. After comparative test analysis, this model could deal with the problem of train speed change more effectively. Yuan's team [2021] proposed an automatic train driving system based on virtual parameter learning to solve the problem that the accuracy of track tracking control of rail trains was not high. After empirical analysis, the system realized accurate tracking and control of train speed and distance track. Jia et al. [2020] proposed a robust nonlinear model predictive control model to handle the issue of low prediction accuracy of nonlinear models in trains. Through comparative test analysis, this algorithm improved the precision of the model. Muniandi [2020] proposed a new blockchain-based virtual coupled railway traffic collision main line train automatic driving system to solve the problem that the operation of rail cars was affected by weather. Through simulation test analysis, this system had advantages in resolving train operation scheme conflicts. To better balance the running speed and safety of urban rail trains, Zhang et al. [2022] proposed an automatic train driving technology based on deep reinforcement. This technology could improve passenger comfort and achieve a better balance between operating efficiency and safety.

The energy consumption of underground rail transit is more complex, and the relevant scholars at home and abroad have gradually in-depth research on it. Zhang et al. [2021] manufactured a wind energy harvesting device based on an elastic rotating triboelectric nanogenerator (ER-TENG), which was used to collect wind energy generated by a high-speed train and power the associated signal and sensing device. The experimental results showed that the energy harvesting efficiency of the ER-TENG was twice that of the conventional rotating-slip triboelectric nanogenerator (RS-TENG), and the durability was four times higher. Isik et al. [2021] used a technology rich, bottom-up energy system optimization model to reduce carbon dioxide emissions from electric vehicles. This model analyzed the cost and air emission impacts of proposed CO2 reduction policies for the transportation sector in New York City through a scenario framework. The analysis showed that early electrification of light vehicles was essential to further reduce air emissions. Meng et al. [2021] found that China's hydrogen energy industry still faced problems such as high comprehensive utilization cost, imperfect hydrogen energy utilization standards and regulations, obvious trend of blind industrial development, and structural overcapacity risk. Therefore, some policy suggestions were put forward for future development, such as strengthening the top-level design, strengthening the pilot demonstration, promoting the development of the whole hydrogen industry chain, and reducing the cost of hydrogen fuel cell vehicles in the field of transportation. Shao et al. [2021] proposed an optimized operation strategy for the integration of electricity and hydrogen for transportation using hydrogen tube trailers. Taking into account the constrained operation of power systems (EPS), transport systems and variable renewables, the proposed strategy harmonized the stages of hydrogen generation, transport and storage. The proposed method was based on alternating direction multiplier (ADMM), which managed the HES and EPS constraints respectively and coordinates their solutions. The experimental results showed that the energy efficiency of the proposed model and its solution was increased by 42.2%. Tardivo et al. [2021] found that transportation played an important role in greenhouse gas emissions during the COVID-19 pandemic. Therefore, it was proposed that the development of green transportation should be flexible, rewarding, reconsidered, reformed, and researched as necessary steps for the railway sector to better continue providing services in future crises.

To sum up, the development of underground rail transit cannot be separated from the support of various high and new technologies, among which automatic train driving technology is widely used in the construction of rail trains. However, nowadays, most scholars pay more attention to the development of underground rail transit in terms of speed, safety and maintenance, but pay less attention to the huge energy consumption of underground rail transit. To fill the data gap in this research direction, this study proposes to optimize the energy-saving technology of underground rail trains by using the control strategy of automatic train driving system. It is hoped that this study can realize the purpose of energy saving of underground rail transit and provide a new research idea for the field of energy saving of rail trains.

3. Research on energy-saving model of underground rail transit combined with micro-field theory

Because of its high speed and high on-time rate, underground rail transit has become one of the important transportation modes for people to travel, which effectively alleviates the pressure of urban traffic. Recently, however, the underground rail's energy consumption has doubled with its expansion. To solve this problem, this chapter applies the control strategy of automatic train driving system to improve the energy-saving technology, and the interval operation model of underground rail train is optimized with the micro-field theory.

3.1. Train energy saving technology based on ATO control strategy

The energy consumption of underground rail trains is mainly affected by traction force, resistance force and braking force [Rautiainen et al., 2021]. Train tractive force refers to the rotating torque produced by the train wheel. The tractive force generation diagram is shown in Fig. 1. In Fig. 1, M_i generates couple F_i and F_i' for the driving torque; The couple F_i causes the wheel to move to the left, creating a force f_i' on the rail and friction f_i, or traction. The tractive force calculation Equation is shown in Equation (1) [Novak H et al. 2021].

$$\begin{cases} F_i = F_i' = M_i / R_i \\ f_i = f_i' = F_i' \times R_i \end{cases} \tag{1}$$

In Equation (1), R_i is the radius of the wheel; When F_i increases, f_i' increases accordingly; The amount of traction is closely related to the speed of the train. The characteristic curve of traction force related to velocity is shown in Fig. 1 (b).

In Fig. 1(b), the tractive force value is inversely proportional to the train running speed, and the tractive force value increases with the increase of the network pressure. The calculation equation of the acceleration and train acceleration is shown in Equation (2).

$$F = (M_m + M_t) \cdot g \cdot a(v, v_{target}) \tag{2}$$

In Equation (2), M_m is the train mass; M_t denotes the mass of the trailer; $a(v, v_{target})$ is the acceleration of the train speed in relation to the target speed; g is the acceleration of gravity. The resistance of the train includes basic resistance and additional resistance, among which the additional resistance is caused by the ramps and bends in the train running line. The calculation equation of additional resistance is shown in Equation (3).

$$w_k = w_0 + w_i + w_r + w_s \tag{3}$$

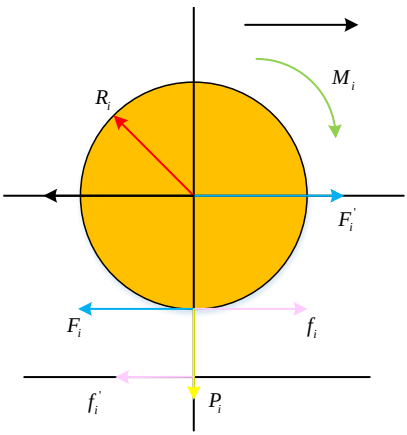

(a) Schematic diagram of traction force generation

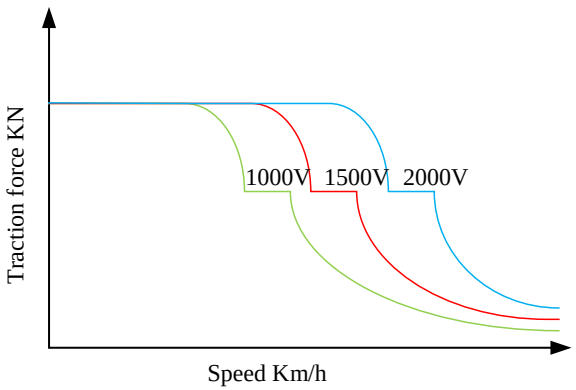

(b) Characteristic curve related to traction and speed

Fig. 1. Traction generation and characteristic curve

In Equation (3), w_k is the additional resistance; w_0 is the basic resistance; w_i is the additional resistance of the ramp; w_r is the additional resistance to the curve; w_s is the additional resistance of the tunnel. The calculation equation of w_0 is shown in Equation (4).

$$w_0 = a_1 + a_2 v + a_3 v^2 \tag{4}$$

In Equation (4), v is the train running speed; w_r, a_2, a_3 are constants. The calculation equation of w_i is shown in Equation (5).

$$\begin{cases} w_{i_1} = sin\,\theta \approx tan\,\theta = i \\ w_{i_2} = \sum i_n \cdot \dfrac{l_n}{L} \end{cases} \tag{5}$$

In Equation (5), w_{i_1} is the additional resistance of the ramp; i is the slope; θ is the Angle between the ramp and the level ground. w_{i_1} is the additional resistance of the ramp when there are multiple ramps; n is the number of multiple ramps; i_n is the slope of ramp n; l_n is the length of the train on ramp n; L denotes the total train length. The calculation equation of w_r is shown in Equation (6).

$$\begin{cases} w_{r_1} = \dfrac{l_r}{L} \cdot \dfrac{600}{R} \\ w_{r_2} = \sum \dfrac{600}{R_{n_1}} \cdot \dfrac{l_{rn_1}}{L} \end{cases} \tag{6}$$

In Equation (6), w_{r_1} is the additional resistance of the curve in a single curve segment; l_r is the length on the curve of the train; R denotes the radius of the curve. w_{r_2} is the additional resistance of the curve when multiple curve segments appear simultaneously; n_1 is the number of trains across the curve; R_{n_1} is the radius of the n_1 curve; l_{rn_1} is the length of the train on curve n_1. In the urban rail transit system, the train adopts the power distribution structure, and the resistance is divided into basic resistance and additional resistance according to the source. Additional resistance is mainly caused by line conditions. The additional resistance of the curve in Equation (6) is affected by many factors, such as the extra friction between the wheel rim and the rail caused by the pressure of the outer (inner) side of the wheel rim, and the longitudinal sliding of the rolling radius of the two wheels on the same axis due to the different length of the rail inside and outside the curve section. The calculation equation of w_s is shown in Equation (7).

$$\begin{cases} w_{s_1} = 0.00013 L_s \\ w_{s_2} = L_s \cdot v^2 / 10^7 \end{cases} \tag{7}$$

In Equation (7), w_{s_1} is the additional resistance of the tunnel when there is no limit ramp in the tunnel; w_{s_2} is the additional resistance to the tunnel when there are restricted ramps in the tunnel; L_s is the length of the tunnel. Common braking of trains is divided into air braking and electrical braking. The mathematical expression of the train's braking dynamic model is shown in Equation (8).

$$b = 1000 \theta_h \varphi_h \tag{8}$$

In Equation (8), θ_h is the converted braking rate of the train; φ_h is the coefficient of friction is converted. In the process of train operation, energy consumption caused by traction is the most significant, and its calculation equation is shown in Equation (9).

$$E = \int_0^T F(t) v(t) dt \tag{9}$$

In Equation (9), T is the total running time; $F(t)$ is the traction force on the train at t time; $v(t)$ is the train speed at time t. To sum up, the key to saving energy in train operation is to reduce the traction of the train or the speed of the train, but meanwhile to meet the on-time rate of the train [Mironiuk W et al. 2023]. Automatic train operation (ATO) system can realize automatic train running, accurate parking and other functions. Therefore, ATO control strategy is proposed to improve the energy-saving technology of train operation. The running process of underground rail trains can be divided into four stages: traction, cruise, idle running and braking, as shown in Fig. 2.

When the train is in traction stage, the energy expenditure generated is the work done by the traction force to overcome the resistance. In the cruise phase, traction equals resistance, and energy consumption is the work that traction does to overcome resistance. In the idling and braking stages, traction does not

produce energy consumption. According to the train operation law and ATO control strategy, the train operation optimization model is established based on train position and speed limit, and its mathematical expression is shown in Equation (10).

$$\begin{cases} min\, E = \int_0^{T_1} f(v(D)) \cdot v(t)dt \\ st. \sum t_i = T_1 \\ \sum s_i = S \\ 0 < s_1 \le s_2 \ldots \le s_j < S \\ 0 \le v \le V_{Li} \\ 0 \le \eta \le 1 \end{cases} \tag{10}$$

In Equation (10), D is the solution of the model; t_i denotes the time of the section in which the train operates; T_1 is the planned running time of the segment; s_i is the running distance; S is the station distance; V_{Li} indicates the zone speed limit value; s_1 to s_j are the locations of the transition points for each working condition; η is the coefficient of use of traction force and braking force. Since this optimization model is a nonlinear problem with single objective and multiple independent variables, GA is applied [Wang et al. 2022]. The solution flow chart is shown in Fig. 3.

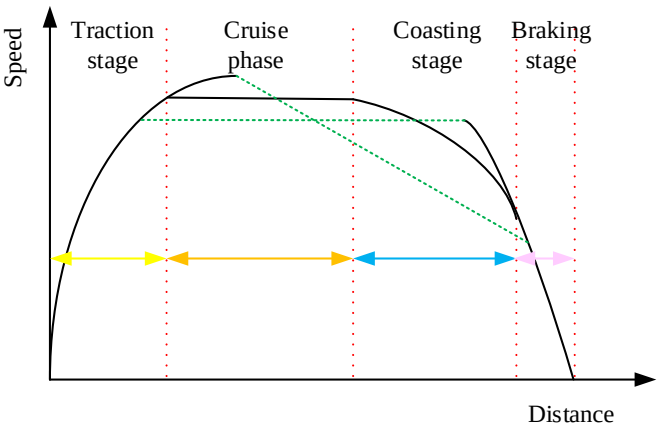

Fig. 2. Four stages of the train operation

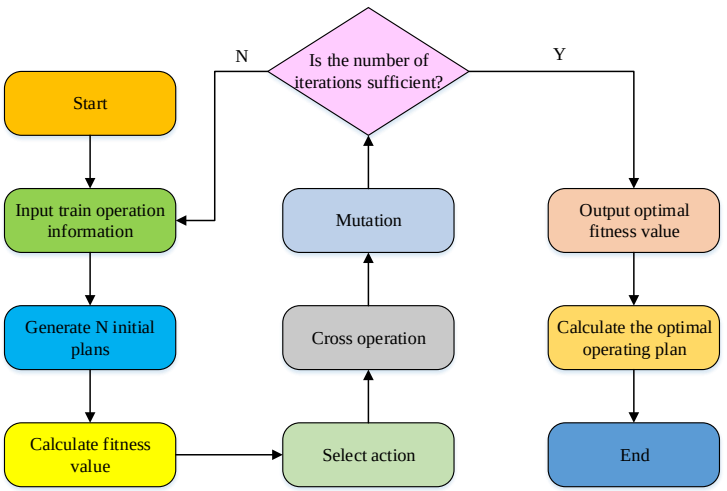

Fig. 3. Flow chart of the optimization model solution

In Fig. 3, the algorithm produces an interval operation scheme based on the basic train parameters, routes and other information, and then constrains the fitness value through the restriction condition of saving train energy consumption. The optimal fitness value is obtained by iterating through four workflows, namely, calculating fitness value, selecting operation, crossing operation and mutation operation. The fitness value can be used to calculate the optimal plan of train operation.

3.2. Energy-saving model of train operation based on Microfield theory

Underground rail transit is composed of many running lines, which are crisscross and complex in structure. And the situation of each running line is different, how to rationally plan the running of trains between each line is essential. Reasonable operation model can not only improve the efficiency of train operation, but also reduce the energy consumption of each line [Yin et al., 2021; Kargwal et al., 2022]. The central idea of field theory is that "a network, or a configuration, of objective relations between various locations". That is, each field has relatively independent autonomy and strong or weak correlation to other fields [Ana et al., 2020; Mccord et al., 2020]. Therefore, field theory is widely used in the field that emphasizes the "relation" Angle. Therefore, the field theory is proposed to optimize the operation of underground rail transit. Each train station is regarded as a field, and quantities of fields form a micro-field. The application of field theory in spatial relations focuses on spatial and external relationships, actors and habitus. The spatial relationship network refers to that each field in the Microfield is an independent space, but closely related to each other. Meanwhile, these Spaces are divided into different levels of subspaces; The complex relationships of subspaces form different network relationships. Actors and habitus refer to the actors with subjective initiative and their behavior habits in the field. In the underground rail transit, the running diagram of all trains can be regarded as "spatial and external relationship network". Passengers and their behavior habits are regarded as "actors and habitus". The operating diagram of underground rail transit trains is divided into single-line operating diagram, double-line operating diagram, single-double line operating diagram, etc. The schematic diagram is shown in Fig. 4

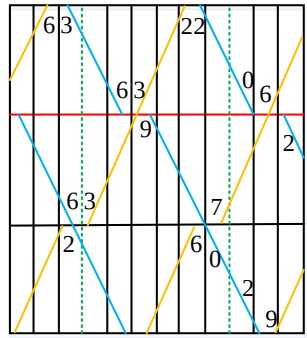

(a) Single line operation diagram

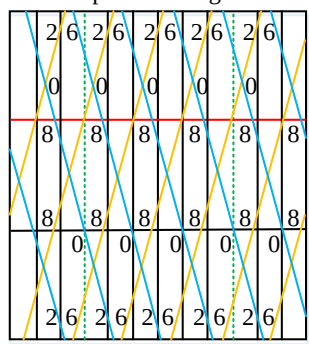

(b) Dual track train diagram

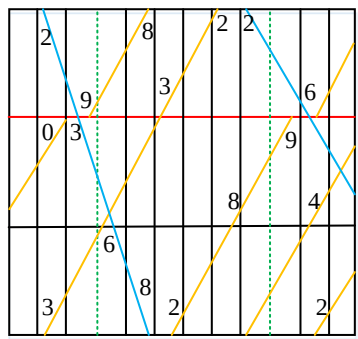

(c) Single and double track operation diagram

Fig. 4. Operation diagram of single line, double line and single line and double line

In Fig. 4, the downward train operation line is from the upper left to the lower right, and the upward train operation line is from the lower left to the upper right. Each box represents time, usually one or two minutes. The ordinate indicates the actual mileage of the train, scaled down. The horizontal lines are divided according to a certain proportion, indicating the center line of the station. Transfer stations and terminals are represented by solid red lines [Zhao et al., 2023; Maheshwari et al., 2022; Srivastava et al., 2022]. Various conditions occurs during the operation of underground rail transit, which are generally divided into common conditions and accidental conditions. Such as travel peak, holidays, weather changes, etc., these conditions affect passenger travel behavior. The specific classification of underground rail transit operating conditions is shown in Fig. 5.

Combined with the running diagram of underground rail transit and the running condition, the optimization model of energy consumption of underground rail transit is constructed by using the micro-field theory. The calculation equations of network line analysis in the model are shown in Equations (11), (12) and (13).

$$C_i^{s'} = \frac{1}{N'-1} \sum_{j=1;j\neq i}^{N'} \frac{d_{ij}^{Eucl}}{d_{ij}} \tag{11}$$

In Equation (11), $C_i^{s'}$ denotes the directness of node i; N' is the number of network nodes; d_{ij}^{Eucl} denotes the Euclidean distance between nodes i and j; d_{ij} denotes the shortest distance between nodes i and j.

$$C_i^{c'} = (N'-1) / \sum_{j=1;j\neq i}^{N'} d_{ij} \tag{12}$$

In Equation (12), $C_i^{c'}$ is the proximity of node i.

$$C_i^{B'} = \frac{1}{(N'-1)(N'-2)} \sum_{j=1;k=1;k\neq i}^{N'} \frac{n_{jk}(i)}{n_{jk}} \tag{13}$$

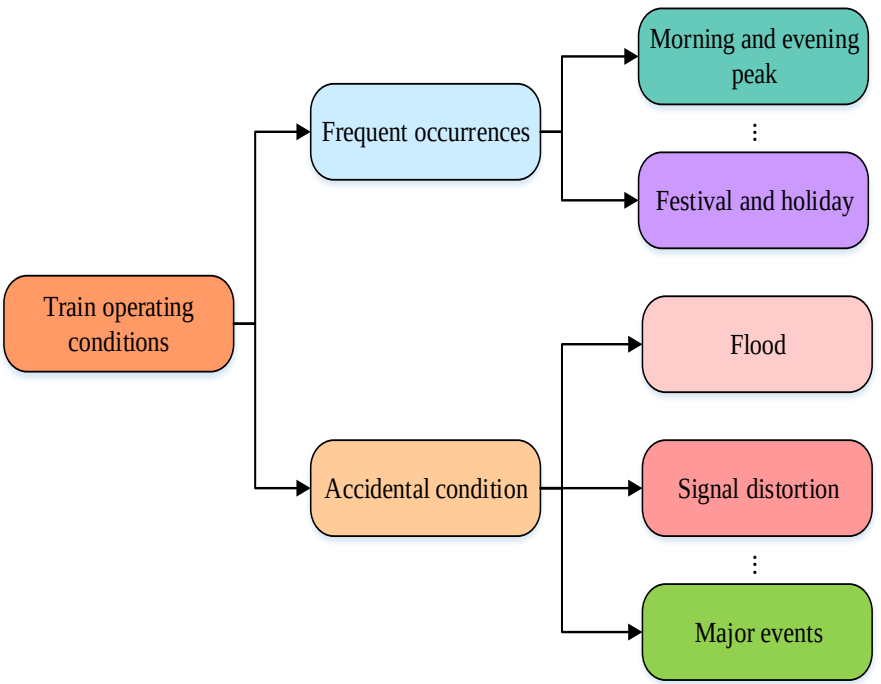

Fig. 5. Operation status of underground rail transit

In Equation (13), $C_i^{B'}$ is the mediation of node i. n_{jk} denotes the number of shortest paths between nodes j and k; $n_{jk}(i)$ denotes the number of shortest paths between nodes j and k passing through node i; In this case, node i denotes the passing point. The calculation equations of spatial density analysis in the model are shown in Equations (14) and (15).

$$f(x) = \frac{1}{n'h}\sum_{i=1}^{n'} K\left(\frac{x - x_i}{h}\right) \tag{14}$$

In Equation (14), $K\left(\frac{x-x_i}{h}\right)$ denotes the kernel density equation; h denotes the threshold value; n' denotes the number of points in the range; $x - x_i$ is the distance from the valuation point x to the event point x_i.

$$I = \frac{N_Z \sum_{i=1}^{N_Z}\sum_{j=1}^{N_Z} C_{ij}(X_i^a - \bar{X}_a)(X_i^b - \bar{X}_b)}{\sum_{j=1}^{N_Z}\sum_{j=1}^{N_Z} C_{ij}\sum_{i=1}^{N_Z}(X_i^a - \bar{X}_a)(X_j^b - \bar{X}_b)} \tag{14}$$

In Equation (15), N_Z denotes the total number of space units; C_{ij} denotes the weight matrix between two spatial units; X_i^a is the value of attribute a in the space; $\bar{X}_a$ is the average value of attributes in the space; X_i^b and X_j^b both represent the value of attribute b in the space; $\bar{X}_b$ is the average value of attributes in the space. The optimization of train energy saving technology and the operation optimization of underground rail transit are integrated. Meanwhile, the basic Settings in the station are optimized, such as lighting, fan and other energy consumption, and the energy-saving model of underground rail transit is built. The model structure is shown in Fig. 6 [Barma and Modibbo, 2022].

In Fig. 6, energy conservation of underground rail transit is mainly optimized from four aspects: train operation, route planning, overall operation planning of rail transit, and infrastructure. Through ATO control strategy and micro-field theory, the research mainly optimizes energy consumption of train energy-saving technology, route planning and overall operation planning of rail transit, and finally realizes the optimal energy saving of underground rail transit.

4. Simulation test analysis of energy-saving model of underground rail transit

To test the application effect of the proposed method. The research applies MATLAB simulation software, and collects the actual basic data of underground rail transit operation in a city for experiment. In this experiment, indicators such as train speed and rail transit line energy consumption are used to evaluate the energy-saving model proposed in the study.

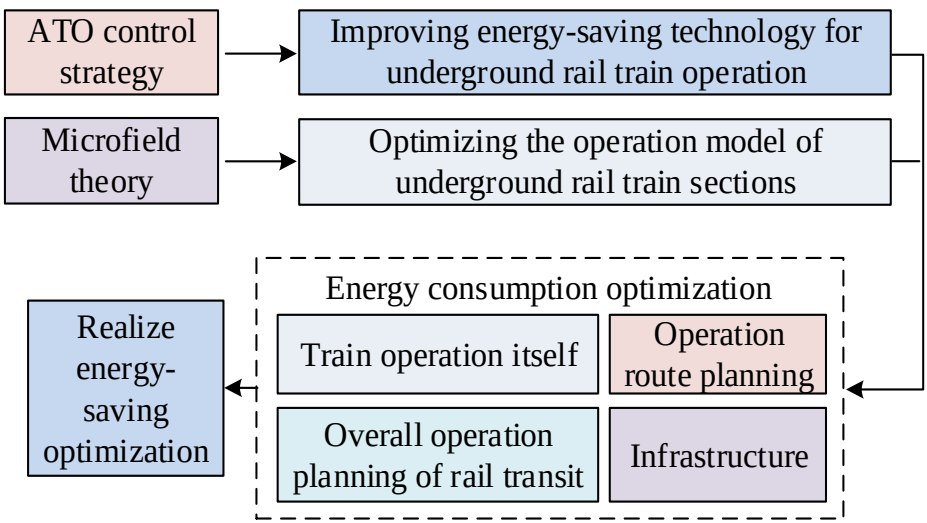

Fig. 6. Energy-saving model of underground rail transit

4.1. Basic test data

The basic information of underground rail trains used in a certain city is collected and screened, and the content required for the test is selected and recorded. Table 1 shows the basic parameters of the trains.

In Table 1, the maximum width of underground rail trains used in this city is 2.9m, the length is 120m, and the self-weight is 198t. The train has a maximum operating speed of 80km/h. The average acceleration is not less than 0.6m/s2. The average deceleration is not less than 1.0m/s2. Emergency deceleration is not less than 1.21.0m/s2. The adhesion coefficients of traction force and braking force are 0.18 and 0.17. When the electric braking function of the train is normal, it is not necessary to use air braking for auxiliary braking. In Table 2, the research test requires not only the basic data of trains, but also the statistics of all running lines and stations in the city.

In Table 2, the research conducts statistics on the underground rail transit lines and stations of the city. The city's underground rail trains cover eight districts of the city, with a total of eight operating lines. Among them, Line 1 has 33 stations, the slope value of the line is -24‰, and the curve speed limit is 70km/h. Line 2 has a total of 44 stations, the slope value of the line is 23‰, and the curve speed limit is 62km/h. Line 3 has 38 stations, the slope value of the line is -21‰, and the curve speed limit is 67km/h. Line 4 has 22 stations, the slope value of the line is 27‰, and the curve speed limit is 73km/h. Line 5 has 31 stations, the slope value of the line is 34‰, and the curve speed limit is 68km/h. Line 6 has a total of 30 stations, the slope value of the line is 30‰, the curve speed limit is 77km/h; Line 7 has 35 stations, the slope value of the line is 31‰, and the curve speed limit is 76km/h. Line 8 has a total of 40 stations, the slope value of the line is -31‰, and the curve speed limit is 74km/h.

Table 1. Basic parameters of the train

Number	Performance/Parameters	Concrete content	Nnit
1	Maximum width of train	2.9	m
2	Train length	120	m
3	Train self weight	198	t
4	Maximum train speed	80	km/h
5	Average acceleration	≥0.6	m/s^2
6	Adhesion coefficient of train traction force	0.18	/
7	Average deceleration of train service braking	≥1.0	m/s^2
8	Average deceleration of train emergency braking	≥1.2	m/s^2
9	Adhesion coefficient of train braking force	0.17	/
10	Train braking characteristics	When the electric braking of the train is normal, the combination does not require Railway air brake	/

Table 2. Basic data of the underground rail transit line in a certain city

Line	Line 1	Line 2	Line 3	Line 4	Line 5	Line 6	Line 7	Line 8	Statistics
Zone A	8	4	4	6	3	/	/	/	25
Zone B	/	10	/	2	9	8	/	9	38
Zone C	10	3	8	4	/	/	7	/	32
Zone D	/	/	/	/	13	/	/	6	19
Zone E	6	4	6	/	/	/	8	12	36
Zone F	/	/	9	10	/	5	5		29
Zone G	/	16	/	/	6	7	/	6	35
Zone H	9	7	11	/	/	10	15	7	59
Total Line	33	44	38	22	31	30	35	40	/
Slope value ‰	-24	23	-21	27	34	30	31	-31	/
Curve speed limit km/h	70	62	67	73	68	77	76	74	/

4.2. Analysis of application effect of energy-saving model of underground rail transit

The train parameters and traffic route data of the city underground rail is taken as the basic data of the experiment. The experiment is divided into three groups, among which the experimental group using the energy-saving model of underground rail transit proposed in the study is group A; The energy saving model of opportunity constraint planning is used in group B. The experimental group without energy-saving model is group C. The test results of the three groups are compared, and the optimization of the train running speed curve is shown in Fig. 7.

In Fig.7, when the speed threshold is limited to 0.8, the actual running state of group A trains changes when running 100m, 200m, 300m, 800m, 900m and 1120m, and the actual train speed is very close to the target speed. The actual running state of group B trains changes at 200m, 850m, 900m and 1130m, and the actual speed of trains is close to the target speed. The actual running state of group C trains changes at 250m, 400m, 900m and 1150m, and the actual speed of trains fluctuates, and there is a certain gap between them and the target speed. In Fig. 7(b), when the speed threshold is limited to 0.5, the actual running state of trains using the model and the actual running state of trains not using the model both fluctuate to some extent. The energy-saving model of underground rail transit proposed in this study is more accurate for train speed control. When the threshold limit is higher, the control effect is better. The test results of average impact rate and energy loss during train operation are shown in Fig. 8. The smaller the average impact rate means that the train runs more smoothly and the passengers in the train are more comfortable.

In Fig. 8, the average impact rate of group A trains during operation is 0.66m/s2km-1; The average impact rate of Group B train during operation is 0.84m/s2km-1. The average impact rate of Group C trains during operation is 1.23m/s2km-1. In Fig. 8 (b), the energy consumption of group A trains during operation is 38kW.h. The energy consumption of Group B trains during operation is 43kW.h. The energy consumption of Group C trains during operation is 47 Kw. h. The energy saving model of underground rail transit proposed in the study minimizes the average impact rate and energy consumption during train operation, which is better than the comparison group.

In Fig. 9, in the group A test, the running time of 8 lines is 69min, 98min, 67min, 42min, 60min, 61min, 70min and 81min respectively, which are all shorter than that of the other two test groups. The energy consumption of the 8 lines during operation is 298kW.h, 394kW.h, 341kW.h, 199kW.h, 280kW.h, 279kW.h, 324kW.h and 367kW.h, respectively, which are lower than the energy consumption of the other two test groups. The energy-saving model proposed in this study can improve the overall line running speed and reduce energy consumption meanwhile. To further determine the stability of the model, a certain number of track operation cases can be extracted from RailNet data set for comparative tests. The time consumed by the model to calculate all cases is taken as the evaluation index, and the test results are shown in Fig. 10.

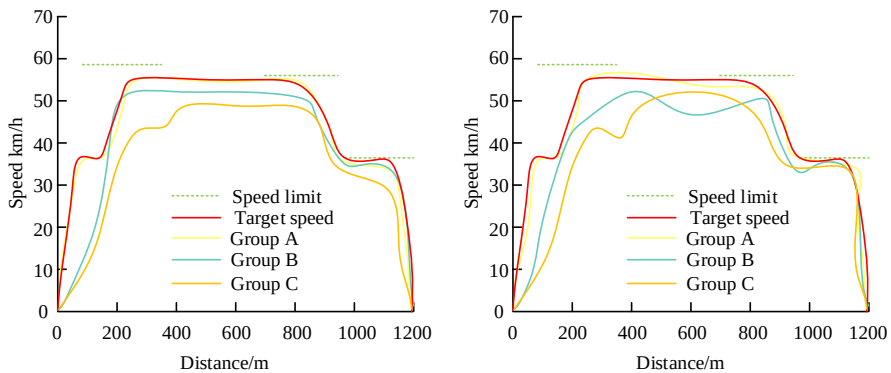

(a) The threshold is 0.8

(b) The threshold is 0.5

Fig. 7. Train running speed curve

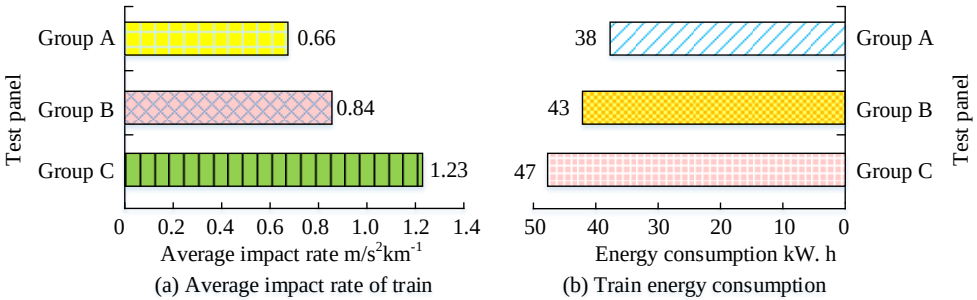

Fig. 8. Average impact rate and energy consumption of trains

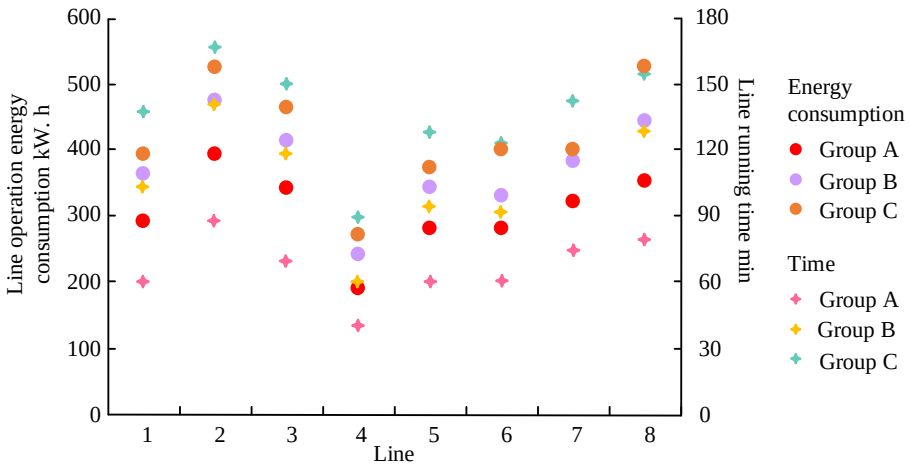

Fig. 9. Running line time and energy consumption

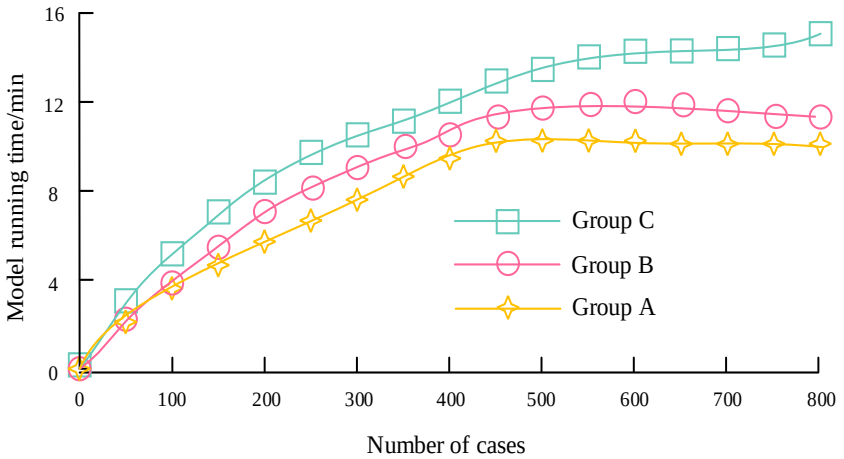

Fig. 10. Model runtime

In Fig. 10, in the test of 0-800 run cases, the operation time of group A model has been maintained at the lowest level. From this time curve, the running time of Group A model is 10min when 450 cases are calculated. Subsequently, with the increase of the number of cases, the calculation time remains basically unchanged. Based on all the above evaluation indexes, the energy-saving model of underground rail transit proposed in this study has the best performance.

5. Analysis of practical application effect of energy-saving model

To test the application effect of the theoretical model designed in the research in the actual scene, the research put it into the subway of A city for a week to analyze the energy-saving effect before and after use. A total of eight lines of the city subway have completed energy-saving tests and debugging, and the subway uses the urban rail transit train traction energy measurement equipment and data analysis platform based on accurate space-time information. Data is collected by sensors in the middle of the train and the final energy consumption is calculated by the device. The energy saving results before and after putting into use are shown in Table 3.

Table 3. Energy saving effects of train operation on various subway lines in City A

Line name	Before investment		After investment	
	Energy consumption (kW. h)	Travel time (min)	Energy consumption (kW. h)	Travel time (min)
1	724.5	93	682.4	80
2	684.9	75	641.0	60
3	648.2	88	598.2	75
4	701.5	84	653.1	71
5	712.5	67	674.6	55
6	682.3	60	632.5	47
7	644.7	98	601.3	81
8	637.5	90	594.8	75

In Table 3, the energy consumption of the eight lines exceeds 600kW.h one week before the model is put into use. After the model is put into use, the energy consumption of the eight lines is reduced by 5.8%, 6.3%, 7.7%, 6.8%, 5.3%, 7.9%, 6.7% and 6.8% respectively. Before it is put into use, the one-way time of each route is more than one hour, and after it is put into use, it is basically reduced by about 10 minutes, and the minimum journey time is 47 minutes. The energy-saving model proposed in the study can effectively reduce the train energy consumption in the practical application process.

6. Discussion

The energy-saving effect and performance of the designed energy-saving model are analyzed through simulation analysis and practical application. From the analysis results, the designed model can effectively reduce energy consumption in subway lines. After putting 8 subway lines in A city into use, the energy consumption of trains decreased by 5.8%, 6.3%, 7.7%, 6.8%, 5.3%, 7.9%, 6.7%, and 6.8%, respectively. From this, the research and design model can effectively reduce energy consumption from the perspective of energy-saving technology. The one-way travel time of the eight routes has also been reduced by 14.0%, 20%, 14.8%, 15.5%, 17.9%, 21.7%, 17.3%, and 16.7%. From this, the energy-saving model designed in the study can help trains plan more suitable scheduling routes and further achieve energy consumption optimization. During the simulation experiment, it is found that the energy-saving train designed in the study has the closest speed to the target speed when the speed threshold limits are 0.8 and 0.5, which is better than the trains in the comparative test group. Moreover, its energy consumption and running time are significantly lower than those in the test group, which indicates that the research designed model can optimize train energy consumption from the overall operational planning of rail transit.

7. Conclusion

Due to the enhancement of underground rail transit, the number of rail routes has doubled, resulting in a large amount of energy waste. Aiming at this situation, this research puts forward the technology of improving train operation energy saving by using automatic train driving control strategy. On this basis, the energy saving model of underground rail transit is built by Microfield theory. To verify the practical application effect of this model, simulation and comparison tests are carried out in the study: the average impact rate and energy consumption of trains using the energy-saving model of underground rail transit proposed in the study are 0.66m/s2km-1 and 38kW.h respectively during operation. When the speed threshold is limited to 0.8 and 0.5, the train speed is closest to the target speed,

which is better than the train in the comparison group. The total running time of the eight tracks using this model is 69min, 98min, 67min, 42min, 60min, 61min, 70min and 81min respectively. The total energy consumption is 298kW.h, 394kW.h, 341kW.h, 199kW.h, 280kW.h, 279kW.h, 324kW.h and 367kW.h, respectively, which are better than the comparison experimental group. To sum up, the energy-saving model proposed in this study compared with the underground rail transit has the best energy-saving effect and good stability, which can provide passengers with a more comfortable travel experience. However, this model is insufficient to study the energy consumption of train infrastructure, such as lighting and air conditioning, which will be a new direction for future research on energy conservation and emission reduction. Developing energy-saving methods for underground rail transit through research and design can help alleviate energy pressure, reduce operating costs of rail transit, and improve operational efficiency. Meanwhile, by implementing energy-saving measures, optimizing train operation speed and scheduling routes, reducing passenger travel time and improving travel efficiency. And by energy-saving train operation, the impact of rail transit on the environment can be further reduced, which is conducive to achieving green and low-carbon development of rail transit.

References

[1] Ana, C., Todeva, E., Carnauba, A., Boaventura, J., & Pereira, C. (2020) Formal and relational mechanisms of network governance and their relationship with trust: substitutes or complementary in Brazilian real estate transactions. *International Journal of Networking and Virtual Organizations*, 22(3), 246-271. https://doi.org/10.1504/IJNVO.2020.10027652.

[2] Barma, M., & Modibbo, U. (2022) Multi-objective mathematical optimization model for municipal solid waste management with economic analysis of reuse/recycling recovered waste materials. *Journal of Computational and Cognitive Engineering*, 1(3), 122-137. https://doi.org/10.47852/bonviewJCCE149145.

[3] Boyacioglu, P., Bevan, A., Allen, P., Bryce, B., & Foulkes, S. (2022) Wheel wear performance assessment and model validation using Harold full scale test rig. *Proceedings of the Institution of Mechanical Engineers, Part F: Journal of Rail and Rapid Transit*, 236(4), 406-417. https://doi.org/10.1177/09544097211022444.

[4] Cai, Y., & Chen, J. (2021) Independent cover is ogeometric Reissner-Mindlin shell model for the simulation of the fabricated lining. *International Journal for Numerical and Analytical Methods in Geomechanics*, 45(17), 2490-2521. https://doi.org/10.1002/nag.3274.

[5] Feng, M., Wu, C., Lu, S., & Wang, Y. (2020) Notch-based speed trajectory optimization for high-speed railway automatic train operation. *Proceedings of the Institution of Mechanical Engineers, Part F: Journal of Rail and Rapid Transit*, 236(2), 159-171. https://doi.org/10.1177/09544097211042184.

[6] Hou, B., Zeng, Q., Fei, L., & Li, J. (2020) Noise evaluation method for urban rail transit underground station platforms. *Journal of Tsinghua University (Science and Technology)*, 61(1), 57-63. https://doi.org/10.16511/j.cnki.qhdxxb.2020.22.019.

[7] Isik, M., Dodder, R & Kaplan, P, O. (2021) Transportation emissions scenarios for New York City under different carbon intensities of electricity and electric vehicle adoption rates. *Nature energy*, 6(1): 92-104. http://dx.doi.org/10.1038/s41560-020-00740-2.

[8] Jia, C., Xu, H., & Wang, L. (2020) Robust nonlinear model predictive control for automatic train operation based on constraint tightening strategy. *Asian Journal of Control*, 24(1), 83-97. https://doi.org/10.1002/asjc.2419.

[9] Kong, L., Wu, Z., Chen, G., Qiu, M., Mumtaz, S., & Podriguse, J. (2020) Crowdsensing based cross-operator switch in rail transit systems. *IEEE Transactions on Communications*, 68(12), 7938-7947. https://doi.org/10.1109/TCOMM.2020.3019527.

[10] Kargwal, R., Kumar, A., Garg, M, K & Chanakaewsomboon, I. (2022) A review on global energy use patterns in major crop production systems. *Environmental Science: Advances*, 2022, 1(5): 662-679. http://dx.doi.org/10.1039/d2va00126h.

[11] Mccord, M., Davis, P., Mccord, J., Haran, M., & Davison, K. (2020) An exploratory investigation into the relationship between energy performance certificates and sales price: A polytomous universal model approach. *Journal of Financial Management of Property and Construction*, 25(2), 247-271. https://doi.org/10.1108/JFMPC-08-2019-0068.
[12] Muniandi, G. (2020) Blockchain-enabled virtual coupling of automatic train operation fitted mainline trains for railway traffic conflict control. *IET Intelligent Transport Systems*, 14(4), 611-619. https://doi.org/10.1049/iet-its.2019.0694.
[13] Meng, X., Gu, A., Wu, X., Zhou, L., Zhou, J., Liu, B & Mao, Z. (2021) Status quo of China hydrogen strategy in the field of transportation and international comparisons. *International Journal of Hydrogen Energy*, 46(57): 28887-28899. http://dx.doi.org/10.1016/j.ijhydene.2020.11.049.
[14] Maheshwari, S., Shetty, S., Ratnakar, R & Sanyal S. (2022) Role of Computational Science in Materials and Systems Design for Sustainable Energy Applications: An Industry Perspective. *Journal of the Indian Institute of Science*, 2022, 102(1): 11-37. http://dx.doi.org/10.1007/s41745-021-00275-9.
[15] Mironiuk W, Buszman K. (2023) Capabilities to use passive measurement systems to detect objects moving in a water region. *Archives of Transport*, 2023, 68(4): 137-156. https://doi.org/10.61089/aot2023.bw74g958.
[16] Novak H, Lešić V, Vašak M. Energy-efficient model predictive train traction control with incorporated traction system efficiency. IEEE Transactions on Intelligent Transportation Systems, 2021, 23(6): 5044-5055.. https://doi.org/10.1109/TITS.2020.3046416.
[17] Rautiainen, M., Remes, H., & Niemel, A. (2021) A traction force approach for fatigue assessment of complex welded structures. *Fatigue and Fracture of Engineering Materials and Structures*, 44(11), 3056-3076. https://doi.org/10.1111/ffe.13548.
[18] Shao, C., Feng, C., Shahidehpour, M., Zhou, Q., Wang, X & Wang, X. (2021) Optimal stochastic operation of integrated electric power and renewable energy with vehicle-based hydrogen energy system. *IEEE Transactions on Power Systems*, 36(5): 4310-4321. http://dx.doi.org/10.1109/tpwrs.2021.3058561.
[19] Srivastava, D., Kapoor, K & Amarendra, G. (2022) Development of Advanced Nuclear Structural Materials for Sustainable Energy Development. *Journal of the Indian Institute of Science*, 102(1): 391-404. http://dx.doi.org/10.1007/s41745-022-00287-z.
[20] Tardivo, A., Carrillo Zanuy, A & Sánchez Martín, C. (2021) COVID-19 impact on transport: A paper from the railways' systems research perspective. *Transportation research record*, 2675(5): 367-378. http://dx.doi.org/10.1177/0361198121990674.
[21] Vickerstaff, A., Bevan, A., & Boyacioglu, P. (2020) Predictive wheel-rail management in London Underground: Validation and verification. *Proceedings of the institution of mechanical engineers, Part F: Journal of Rail and Rapid Transit*, 234(4), 393-404. https://doi.org/10.1177/095440971987861.
[22] Wang, Q., Xi, H., Deng, F., Cheng, M., & Buja, G. (2022) Design and analysis of genetic algorithm and BP neural network based PID control for boost converter applied in renewable power generations. *IET Renewable Power Generation*, 16(7), 1336-1344. https://doi.org/10.1049/rpg2.12320.
[23] Wen, Y., Leng, J., Yu, F., & Yu, C. (2020) Integrated design for underground space environment control of subway stations with atriums using piston ventilation. *Indoor and Built Environment*, 29(9), 1300-1315. https://doi.org/10.1177/1420326X20941.
[24] Xu, S., Wang, H., Tian, X., Wang, T., & Tanikawa, H. (2021) From efficiency to equity: Changing patterns of China's regional transportation systems from an in-use steel stocks perspective. *Journal of Industrial Ecology*, 26(2), 548-561. https://doi.org/10.1111/jiec.13203.
[25] Yang, H., Xu, T., Chen, D., Yang, H., & Pu, L. (2020) Direct modeling of subway ridership at the station level: a study based on mixed geographically weighted regression. *Canadian Journal of Civil Engineering*, 47(5), 534-545. https://doi.org/10.1139/cjce-2018-0727.
[26] Yuan, Z., Yan, L., Gao, Y., Zhang, T., & Gao, S. (2021) Virtual parameter learning-based adaptive control for protective automatic train operation. *IEEE Transactions on Intelligent Transportation Systems*, 22(12), 7943-7954. https://doi.org/10.1109/TITS.2021.3066447.

[27] Yin, Y & Zhang, Y. (2021) Environmental pollution evaluation of urban rail transit construction based on entropy weight method. *Nature Environment and Pollution Technology*, 20(2): 819-824. http://dx.doi.org/10.46488/nept.2021.v20i02.044.
[28] Zhan, S., Sunindijo, R., Loosemore, M., Wang, S., Gu, Y., & Li, H. (2021) Identifying critical factors influencing the safety of Chinese subway construction projects. *Engineering Construction and Architectural Management*, 28(7), 1863-1886. https://doi.org/10.1108/ECAM-07-2020-0525.
[29] Zhang, L., Leong, H., Zhou, M., & Li, Z. (2022) An intelligent train operation method based on event-driven deep reinforcement learning. *IEEE Transactions on Industrial Informatics*, 18(10), 6973-6980. https://doi.org/10.1109/TII.2021.3138098.
[30] Zhu, C., Du, G., Jiang, X., Huang, W., Zhang, D., & Fan, M. (2021) Dual-objective optimization of maximum rail potential and total energy consumption in multi-train subway systems. *IEEE Transactions on Transportation Electrification*, 7(4), 3149-3162. https://doi.org/10.1109/TTE.2021.3062706.
[31] Zhang, C., Liu, Y., Zhang, B., Yang, O., Yuan, W., He, L & Wang, Z, L. (2021) Harvesting wind energy by a triboelectric nanogenerator for an intelligent high-speed train system. *ACS Energy Letters*, 6(4): 1490-1499. http://dx.doi.org/10.1021/acsenergylett.1c00368.
[32] Zhao, W., Xu, J., Fei, W., Liu, Z., He, W & Li, G. (2023) The reuse of electronic components from waste printed circuit boards: a critical review. *Environmental Science: Advances*, 2(2): 196-214. http://dx.doi.org/10.1039/d2va00266c.